Fermi National Accelerator Laboratory

FERMILAB-Pub-96/265-A

Large Angular Scale CMB Anisotropy Induced by Cosmic Strings

B. Allen[1], R. R. Caldwell[2], E. P. S. Shellard[2], A. Stebbins[3], and S. Veeraraghavan[4]
[1] *Department of Physics, University of Wisconsin - Milwaukee, P.O. Box 413, Milwaukee, Wisconsin 53201, U.S.A.*
[2] *University of Cambridge, D.A.M.T.P. Silver Street, Cambridge CB3 9EW, U.K.*
[3] *NASA/Fermilab Astrophysics Center, P.O. Box 500, Batavia, Illinois 60510, U.S.A.*
[4] *NASA/Goddard Space Flight Center, Greenbelt, Maryland 20771*

We simulate the anisotropy in the cosmic microwave background (CMB) induced by cosmic strings. By numerically evolving a network of cosmic strings we generate full-sky CMB temperature anisotropy maps. Based on 192 maps, we compute the anisotropy power spectrum for multipole moments $\ell \leq 20$. By comparing with the observed temperature anisotropy, we set the normalization for the cosmic string mass-per-unit-length μ, obtaining $G\mu/c^2 = 1.05^{+0.35}_{-0.20} \times 10^{-6}$, which is consistent with all other observational constraints on cosmic strings. We demonstrate that the anisotropy pattern is consistent with a Gaussian random field on large angular scales.

PACS numbers: 98.80.Cq, 11.27.+d, 98.70.Vc

Operated by Universities Research Association Inc. under Contract No. DE-AC02-76CH03000 with the United States Department of Energy

Disclaimer

Distribution

Cosmic strings are topological defects which may have formed in the very early universe and may be responsible for the formation of large scale structure observed in the Universe today [1]. In order to test the hypothesis that the inhomogeneities in our universe were induced by cosmic strings one must compare observations of our universe with the predictions of the cosmic string model. This *Letter* presents results of detailed computations of the large angular scale cosmic microwave background (CMB) anisotropies induced by cosmic strings [2]. These predictions are compared to the large scale anisotropies observed by the COsmic Background Explorer (COBE) satellite. Because the predicted temperature perturbations are proportional to the dimensionless quantity $G\mu/c^2$ where G is Newton's constant and c the speed of light, one may constrain the value of μ, the mass per unit length of the cosmic strings. We believe that our estimate of μ is the most accurate and reliable to date.

Our methodology for computing the large angle anisotropy is to simulate the evolution of random realizations of a cosmic string network [3]. From these network simulations we construct the temperature anisotropy pattern seen by various observers within the simulation volume. We have evolved the strings from a redshift $z = 100$ to the present, in a cubical box whose side length is twice the Hubble radius at the end of the simulation. This large box assures that the anisotropy pattern is unaffected by the finite simulation volume.

In order to obtain the large dynamic range required for these simulations we have used a new technique whereby the number of segments used to represent the string network decreases as the simulation proceeds. We have conducted tests of this method by comparing smaller simulations, with and without decreasing the number of segments: the average long string energy density is unaffected; the distribution of coherent velocities (the string velocity averaged over a particular length scale) is preserved down to scales smaller than 1/100 of the horizon radius; the effective mass-per-unit-length of string (the energy in string averaged over a particular length scale) is preserved down to scales smaller than 1/100 of the horizon radius. The decrease in the number of segments was regulated so that on the angular scales of interest the simulation provided a good representation of the cosmic string network. Here we are interested in comparing with data from the COBE Differential Microwave Radiometer (DMR) which measures the anisotropy convolved with an approximately 7° FWHM beam [4]. Our contact with this data is through COBE's predicted correlation function at the 10° angular scale.

The temperature patterns are computed using a discretized version of the integral equation

$$\frac{\Delta T}{T}(\hat{n}, x_{\rm obs}) = \int d^4x\, G^{\mu\nu}(\hat{n}, x_{\rm obs}, x)\Theta_{\mu\nu}(x) \qquad (1)$$

where $\Theta_{\mu\nu}$ is the stress-energy tensor of the string at 4-position x, $x_{\rm obs}$ is the 4-position of the observer, and $\hat{n}$ indicates the direction of the arrival of photons on the celestial sphere. Our results apply only if the present spatial curvature and cosmological constant are small since we use a Green's function $G^{\mu\nu}$ appropriate to a matter-dominated Einstein-deSitter cosmology [5]. While the universe is not entirely matter-dominated at redshifts close to recombination ($z_{\rm rec} \approx 1100$), the approximation is justified because we show below that the large-scale anisotropies are primarily produced at $z \lesssim 100$. Hydrodynamical effects at recombination, which only slightly affect the large angle anisotropy, are not included here. Instead we assume that that the photons are comoving with the dark matter at recombination. We have used the ansatz of local compensation [6] as the initial condition for the perturbations of the matter distribution.

We have generated three independent realizations of the cosmic string network. For each realization we have computed the fractional CMB temperature perturbation, $\frac{\Delta T}{T}(\hat{n}, x_{\rm obs})$, in 6144 pixel directions, $\hat{n}$, on the celestial

sphere of 64 observers distributed uniformly throughout each simulation box. This computational scheme gives $\frac{\Delta T}{T}$ smoothed on about the size of the pixels which are 3.5° or smaller [7]. One of these temperature maps is shown in figure 1. This temperature map has been smoothed with a 10° FWHM beam to permit direct comparison with the published COBE sky maps (http : //www.gsfc.nasa.gov/astro/cobe/dmr_image.html). Note that these published maps have structure on angular scales smaller than 10°; this is receiver noise.

Each temperature map may be expressed in terms of the scalar spherical harmonics $Y_{\ell m}$ on the sphere:

$$\frac{\Delta T}{T}(\hat{n}, x_{\rm obs}) = \sum_{\ell=0}^{\infty} \sum_{m=-\ell}^{\ell} a_{\ell m}(x_{\rm obs}) Y_{\ell m}(\hat{n}). \qquad (2)$$

In this *Letter* we only consider coefficients $a_{\ell m}$ with $\ell \leq 20$. For $\ell > 20$ the error due to finite pixel size and gridding effects is larger than 10%. In reference [7] we consider how to correct the large ℓ harmonics for discretization effects.

For each map we construct the multipole moments

$$\widehat{C}_\ell = \frac{1}{2\ell+1} \sum_{m=-\ell}^{\ell} |a_{\ell m}(x_{\rm obs})|^2. \qquad (3)$$

The monopole and dipole moments ($\ell = 0, 1$) are discarded because they contain no useful information. The mean and variance of $\ell(\ell+1)\widehat{C}_\ell$ for $2 \leq \ell \leq 20$ is plotted in figure 2 in units of $(G\mu/c^2)^2$. We see that the mean spectrum is roughly flat, with $\ell(\ell+1)\widehat{C}_\ell \sim 350(G\mu/c^2)^2$ for $\ell \lesssim 20$.

The standard estimator for the ensemble-averaged correlation function $\widehat{C}(\gamma)$ of $\frac{\Delta T}{T}$ at angle γ may be expressed in terms of the $\widehat{C}_\ell$. We smooth the temperature pattern first with the average DMR beam model window function G_ℓ (tabulated values are given in [8]) which is approximately a 7° beam, and second with a 7° FWHM Gaussian window function $W_\ell(7°)$, for an effective smoothing on angular scales $\theta_{\rm smooth} = 10°$.

$$\widehat{C}(\gamma, 10°) = \sum_{\ell=2}^{20} \frac{2\ell+1}{4\pi} \widehat{C}_\ell \, |G_\ell|^2 |W_\ell(7°)|^2 \mathrm{P}_\ell(\cos\gamma)$$

$$W_\ell(\theta) = \exp\Big(-\frac{\ell(\ell+1)}{\ln 2} \sin^2\frac{\theta}{4}\Big) \qquad (4)$$

Here the P_ℓ are Legendre polynomials. By neglecting $\ell > 20$ we would underestimate this sum for $\theta_{\rm smooth} < 10°$. We compute the correlation $\widehat{C}(0°, 10°)$ at the angle $\gamma = 0°$ from our cosmic string simulations and compare it with the same quantity as estimated by the COBE team from the COBE data.

We expect that most of the anisotropy on a particular angular scale is seeded by the strings near the time when the projection of the coherence length of the string network subtends that angle on the celestial sphere [9,10,11,12]. Since the coherence length of the string network grows with time, we expect anisotropies on small angular scales to be seeded at early times, and the large angle anisotropies to be seeded at late times. We have constructed temperature maps which include only a part of the temporal evolution of the string network, from a redshift z to the present. By considering the convergence of $\widehat{C}(0°, 10°)$ as z increases we may determine what redshift range is required to accurately determine $\widehat{C}(0°, 10°)$. In figure 3 we plot the average value of $\widehat{C}(0°, 10°)$ in units of $(G\mu/c^2)^2$ for 64 observers in each of three string simulations as a function of z. We see that $\widehat{C}(0°, 10°)$ receives its dominant contribution within a redshift $z \sim 20$, although there is continued growth through $z \sim 100$. Two independent models of the temperature correlation function indicate that by neglecting the contribution of cosmic strings in the redshift range $100 < z < z_{\rm rec}$ we underestimate $\widehat{C}(0°, 10°)$. The underestimate in the smoothed autocorrelation function is 18% according to the semi-analytic model of Bennett *et al* [10], and 25% according to the analytic model of Perivolaropoulos [11]. We use the latter, more conservative model to extrapolate our results, valid to $z = 100$, out to the redshift of recombination.

We may normalize the cosmic string mass per unit length, μ, by matching estimates of $\widehat{C}(0°, 10°)$ from COBE-DMR with our predictions. The COBE-DMR four year sky maps yield $\widehat{C}(0°, 10°) = (29 \pm 1\,\mu\mathrm{K}/T)^2$ [13] with mean temperature $T = 2.728 \pm 0.002\,\mathrm{K}$ [14]. Our simulations indicate that at $z = 100$, $\widehat{C}(0°, 10°) = 82 \pm 19(G\mu/c^2)^2$ where the ± 19 gives the cosmic variance between the different observers in all three of our simulations. The analytic model [11] predicts that at $z_{\rm rec}$, $\widehat{C}(0°, 10°) = 103 \pm 24 \pm 20(G\mu/c^2)^2$, where the ± 24 is the new cosmic variance. The ± 20 is a conservative systematic error composed of a $\sim 10\%$ uncertainty due to the simulation technique of reducing the number of string segments, $\sim 7\%$ due to the difference in the two models used for the extrapolation out to z_{rec}, and $\sim 5\%$ due to the discretization of the celestial sphere. (These errors will be discussed in more detail in [7].) Note that our result is not strongly dependent on the extrapolation out to $z_{\rm rec}$, which makes only a small correction, lowering the normalization of μ by 10%, in comparison to the quoted uncertainties. Hence, adding these errors linearly, normalization to COBE yields

$$G\mu/c^2 = 1.05^{+0.35}_{-0.20} \times 10^{-6} \qquad (5)$$

for the cosmic string mass per unit length.

Because the spatial distribution of the cosmic string network is not described by Gaussian random variables, we expect that the anisotropy pattern generated in the cosmic string scenario will be non-Gaussian at some level. At very small angular scales, the sharp temperature dis-

continuities across strings guarantee non-Gaussian features. One might hope to find a non-Gaussian signature to distinguish cosmic string models from inflationary models, for which the anisotropy patterns are expected to be very Gaussian. On the large DMR angular scales we are studying, however, we will see that many different strings contribute significantly to each resolution element of the temperature pattern, so the conditions for the central limit theorem are very well satisfied and the temperature pattern is very close to Gaussian.

We have looked for non-Gaussianity in the distribution function of the temperature anisotropy after smoothing our maps with the average DMR beam [8] model window function, an approximately 7° Gaussian beam. The distribution function after combining all of our maps is shown in figure 4. We see that the distribution, on angular scales accessible to DMR, is very close to a Normal distribution. The pixel temperature distribution for any such single observer will not appear as smooth, just as for a limited sample drawn from a true Normal distribution.

It has been suggested that the distribution of temperature differences is a better test of non-Gaussianity than the temperature distribution [15,16]. In figure 5 we plot the distribution of the differences in temperature of nearby pixels. We see that for temperature differences on angular separations greater than the COBE DMR 7° angular resolution scale, the distribution of temperature differences is again very close to a Normal distribution. With finer angular resolution than that probed by DMR, as may be possible with the MAPS or COBRAS/SAMBAS detectors, the inherently non-Gaussian character of the temperature anisotropy due to cosmic strings may be observed. We shall further examine this and other aspects of the map statistics in reference [7].

In this *Letter* we have presented the first computation of large angle CMB anisotropy from cosmic strings which has included all of the relevant physics. Our normalization of μ (5) is consistent with most previous work. Existing studies of the expected large-scale CMB anisotropies find $G\mu/c^2 = 1.5(\pm 0.5) \times 10^{-6}$ [10] and $1.7(\pm 0.7) \times 10^{-6}$ [11] (also see [12]). Note that our results do not appear consistent with Coulson *et al* [16], who obtain the higher normalization $G\mu/c^2 = 2 \times 10^{-6}$ (they quote no uncertainties). They use the lattice-based Smith-Vilenkin evolution algorithm in Minkowski spacetime to produce 18 realizations of a 30° square patch temperature field. Our results should be more accurate because: we simulate the string motion in an expanding universe; our simulation allows smooth variation of quantities such as the string's velocity; our 192 full-sky realizations are comparable to over 8800 30° patches and thus have better statistics. Our normalization of μ is also compatible with other observational constraints on cosmic strings. The bound on gravitational radiation due to pulsar timing residuals and primordial nucleosynthesis gives $G\mu/c^2 < 5.4(\pm 1.1) \times 10^{-6}$ [17]. The bound due to cosmic rays emitted by evaporating primordial black holes formed from collapsed cosmic string loops gives $G\mu/c^2 < 3.1(\pm 0.7) \times 10^{-6}$ [18]. CMB fluctuations on angular scales below 10 arc-seconds gives $G\mu/c^2 < 2 \times 10^{-6}$ at the 95% confidence level, assuming no reionization [19]. The normalization presented in this *Letter* should allow a more direct confrontation of the cosmic string model with observations of large scale density inhomogeneities.

ACKNOWLEDGMENTS

We thank the LASP at NASA/Goddard Space Flight Center for use of computing resources. The work of BA was supported by NSF grants PHY91-05935 and PHY95-07740. The work of RRC and EPSS was supported by PPARC through grant GR/H71550. The work of AS was supported by the DOE and by NASA under grant NAGW-2788. The work of SV was supported by the NRC at Goddard.

REFERENCES

[1] A. Vilenkin, Phys. Rep. **121**, 263 (1985); A. Vilenkin and E. P. S. Shellard, *Cosmic Strings and other Topological Defects*, (Cambridge University Press, Cambridge, England, 1994); M. Hindmarsh and T.W.B. Kibble, Rep. Prog. Phys. **58**, 47 (1995).

[2] B. Allen *et al.*, in *CMB Anisotropies Two Years After COBE*, ed. L. Krauss (World Scientific, New York, 1993).

[3] B. Allen and E. P. S. Shellard, Phys. Rev. Lett. **64**, 119 (1990).

[4] G. Smoot *et al.*, Ap. J **360**, 685 (1990).

[5] S. Veeraraghavan and A. Stebbins, in preparation (1996).

[6] S. Veeraraghavan and A. Stebbins, Ap. J. **365**, 37 (1990).

[7] B. Allen *et al.*, in preparation (1996).

[8] E. L. Wright *et al.*, Ap. J **420**, 1 (1994).

[9] F. Bouchet, D. Bennett, and A. Stebbins, Nature **355**, 410 (1988).

[10] D. Bennett, A. Stebbins, and F. Bouchet, Ap. J. Lett. **399**, L5 (1992);

[11] L. Perivolaropoulos, Phys. Lett. **B298**, 305 (1993).

[12] T. Hara, P. Mahonen, and S. Miyoshi, Ap. J. **414**, 421 (1993).

[13] A. Banday *et al.* COBE Preprint 96-04 astro-ph/9601065 (1996).

[14] C. Bennett *et al.* COBE Preprint 96-01 astro-ph/9601067 (1996).

[15] R. Moessner, L. Perivolaropoulos, and R. Brandenberger, Ap. J. **425**, 365 (1994); P. Graham, N. Turok, P. Lubin, and J. Schuster, Ap. J. **449**, 404 (1995).

[16] D. Coulson, P. Ferreira, P. Graham, and N. Turok, Nature **368**, 27 (1994).

[17] R. R. Caldwell, R. A. Battye, and E. P. S. Shellard, University of Cambridge Preprint DAMTP-R96-21, astro-ph/9607130.

[18] R. R. Caldwell and Paul Casper, Phys. Rev. **D53**, 3002 (1996).
[19] Mark Hindmarsh, Ap. J. **431**, 534 (1994).

FIGURES

FIG. 1. The temperature anisotropy map for one of 192 realizations of the cosmic string induced CMB anisotropy patterns which we have generated for this *Letter*. This is an equal area, all-sky map using a Hammer-Aitoff projection. The map has been smoothed with a 10° FWHM Gaussian beam.

FIG. 2. Plotted is the $\ell(\ell+1)\widehat{C}_\ell$ angular power spectrum for the anisotropies from our realizations. The central dot gives the mean for all 192 observers while the symmetric error bars give the rms variation between different observers.

FIG. 3. Plotted is the rms anisotropy after smoothing with an effective 10° smoothing beam versus the maximal redshift, z, for which strings have been included. The different curves give the mean value of rms anisotropy averaged over the 64 observers in each of the three cosmic string simulations. Local compensation has been applied at each starting time.

FIG. 4. Plotted is the frequency of temperature anisotropy for all pixels in each of our 192 maps after smoothing with a model of the average DMR beam, an approximately 7° Gaussian beam. The solid line gives a Normal distribution with zero mean and variance determined by the pixel distribution amplitude.

FIG. 5. Plotted is the frequency of temperature differences for all pairs of pixels at a given angular separation in each of our 192 maps with no smoothing. The lines show a Normal distribution with variance determined by the pixel difference distribution amplitudes. The three pairs of curves with increasing variance are for separations spanning the ranges $10° \pm 1°$, $20° \pm 1°$, and $40° \pm 1°$.

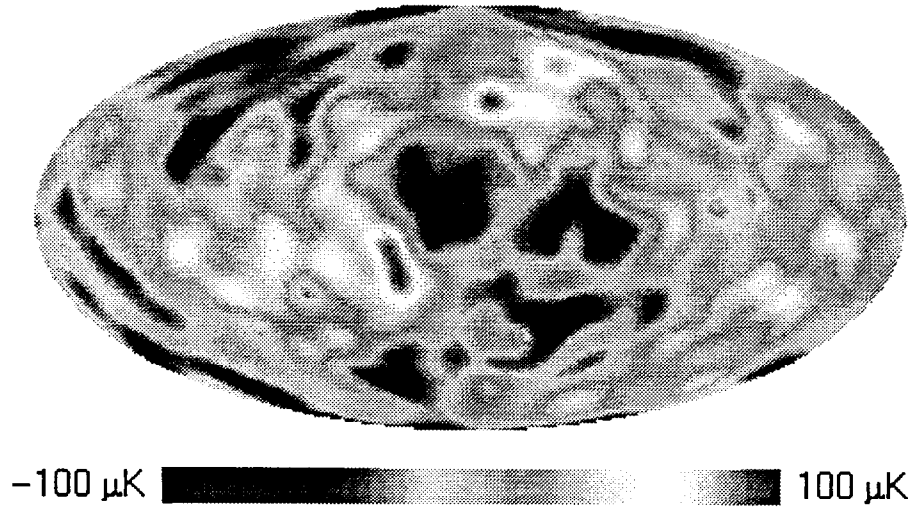

Figure 1.

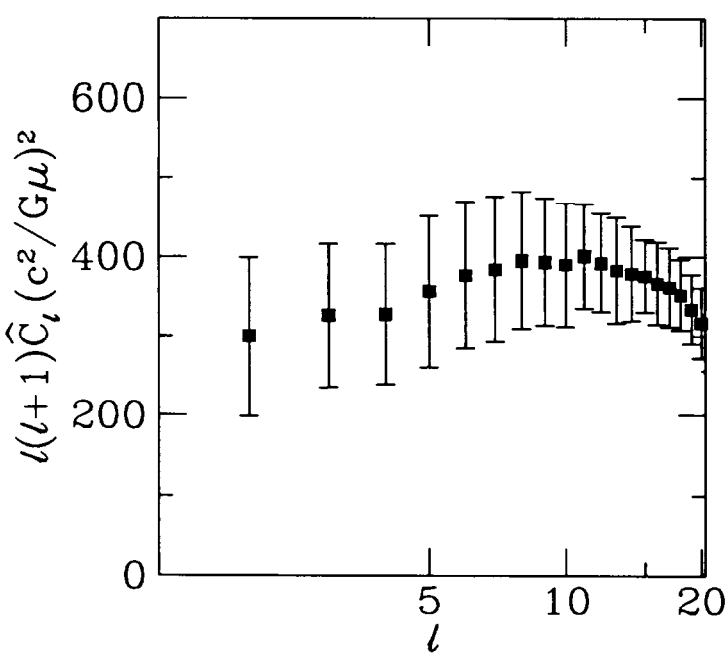

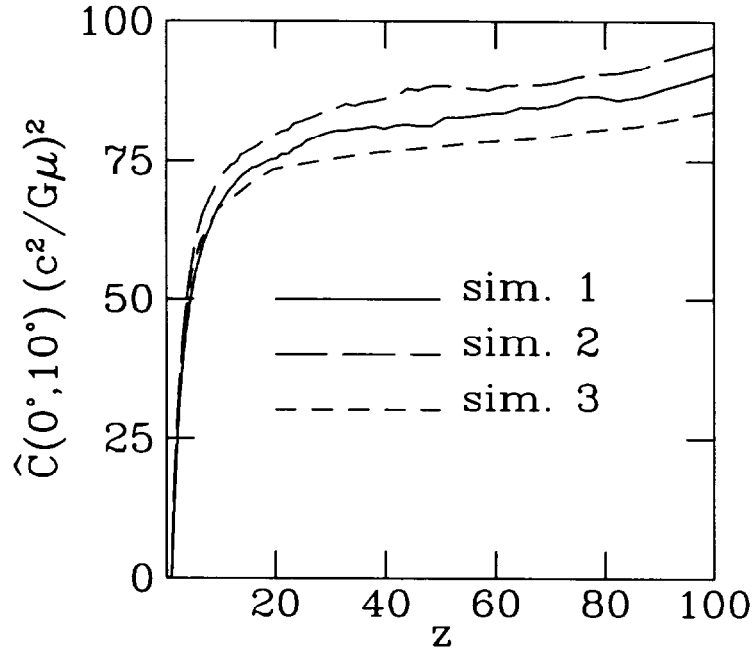

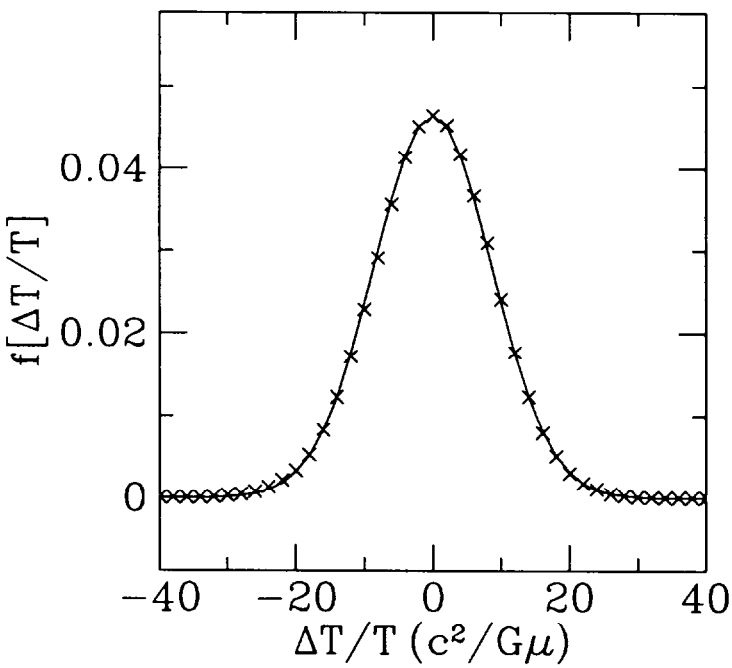

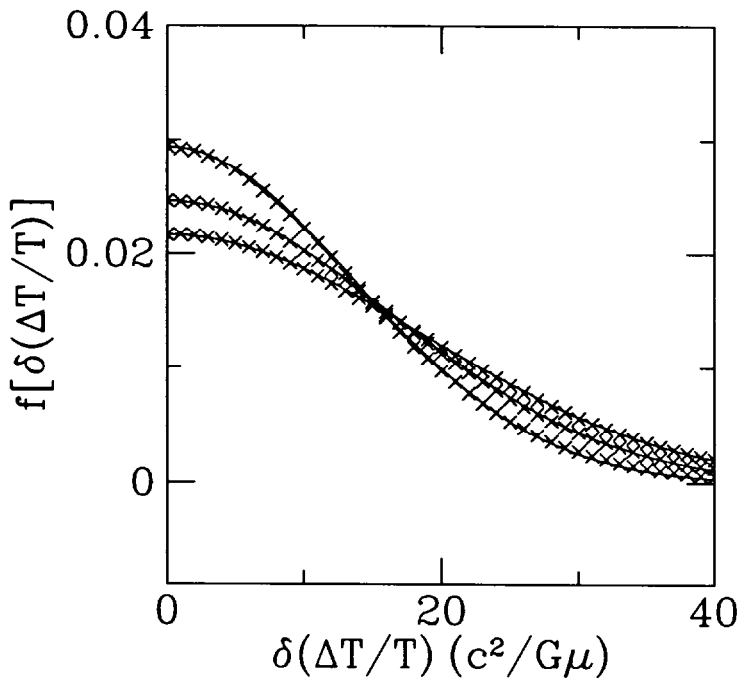

Figures 2 - 3 -4 - 5